HHS Public Access
Author manuscript
Int J Min Reclam Environ. Author manuscript; available in PMC 2015 August 28.

Published in final edited form as:
Int J Min Reclam Environ. 2015 April 7; 2015: .

A study of leakage rates through mine seals in underground coal mines

Steven J. Schatzel[a,*], **Robert B. Krog**[b], **Andrew Mazzella**[a], **Cynthia Hollerich**[a], and **Elaine Rubinstein**[a]

[a]NIOSH, Pittsburgh, PA, USA

[b]West Virginia University, Morgantown, WV, USA

Abstract

The National Institute for Occupational Safety and Health conducted a study on leakage rates through underground coal mine seals. Leakage rates of coal bed gas into active workings have not been well established. New seal construction standards have exacerbated the knowledge gap in our understanding of how well these seals isolate active workings near a seal line. At a western US underground coal mine, we determined seal leakage rates ranged from about 0 to 0.036 m^3/s for seven 340 kPa seals. The seal leakage rate varied in essentially a linear manner with variations in head pressure at the mine seals.

Keywords

mine ventilation; coal mining; mine seals; coal bed emissions; mine safety

Introduction

Overview of mine seals in US coal mines

Seals are widely used in underground US coal mines to isolate mined-out workings, thereby reducing the ventilation load for the mine. With increased longwall panel sizes being realised by current mining equipment, large, mined-out areas of coal mines must be either ventilated or isolated from active workings by mine seals. Areas behind mine seals can be very expansive, potentially consisting of multiple longwall panel gobs or mined-out areas of super sections with pillared, high-extraction areas. In general, sealed mine sections are typically designed to become inert over time as coal bed gas is emitted from the coal and the oxygen component is diminished through oxidation or leakage. Consequently, mine seals are designed to isolate active workings from mined-out sections that are rich in gases emitted from the coal bed and depleted in oxygen.

*Corresponding author. Zia6@cdc.gov.

Disclosure statement
No potential conflict of interest was reported by the authors.

Background

Two mining disasters during 2006 had a profound effect on mining law in the US. The first of these events was the methane explosion at the Wolf Run Mining Company's Sago Mine which resulted in 12 fatalities and one injury in January 2006 [1]. Later in 2006, the Darby No. 1 Mine experienced a methane explosion which killed five workers and injured another [2]. A common element in these two explosions was the close proximity of mine seals that isolated mined-out workings to the active work sites where the miners were killed or injured. Methane–air mixtures behind the seals were ignited either within the mined-out, isolated workings or at the seal line interface. As a consequence of both mine explosions, the seal lines were heavily damaged and were no longer functional as ventilation structures.

A National Institute for Occupation Safety and Health (NIOSH) investigation of mine seal design resulted in a publication by Zipf et al. [3]. This research presented data on the explosive force of methane–air mixtures and demonstrated the inadequacy of the pre-2007 design standard of 140 kPa (20 psi) to withstand the energy associated with a mine explosion. The authors recommended a new set of design parameters for underground mine seals. These research recommendations were largely adopted by US coal mining regulators and were included in new law that was covered in the revised regulation [4]. The regulations greatly increased the structural strength requirements of underground mine seals from the previous 140 kPa (20 psi) standard. The new design parameters allow mine operators to choose from more than one design strength standard and monitoring requirement, but did not address acceptable rates of leakage through the higher strength mine seals. Leakage rates were determined for the prior 140 kPa (20 psi) seal standard and the performances for a variety of seal designs had been reported for testing conducted at a limestone mine [5].

Although the strength of US mine seals has been greatly increased in the US since the Mine Improvement and New Emergency Response Act (MINER Act) of 2006, some questions regarding mine seal performance remain unanswered. Many US coal mine operators have chosen to install the 830 kPa (120 psi) design option (instead of the 340 kPa (50 psi) option) which requires only periodic monitoring of the gas composition behind the mine seal through a sample pipe. Under these circumstances, the gas composition behind seals is not well established and changes in gas composition behind the seals are poorly defined, due to the limited sampling frequency and the lack of reported data from these sites. No leakage rates around or through 340 or 830 kPa (50 or 120 psi) seals have been reported. Many factors have been forwarded as possible influences on seal leakage rates but few measurements have been available to evaluate their individual contribution. The contraction and expansion of gases in mine gobs due to changes in barometric pressure have been documented and may be the most established factor affecting mine seal leakage rates [6,7].

Problem statement

NIOSH configured a research study which was designed to utilise instrument-based data from field monitoring sites to investigate mine seal leakage rates in underground coal mines. Field monitoring included continuous measuring and recording equipment installed on a set of mine seals, in the adjacent airways and at the surface. A key objective of the study was to measure leakage rates through the mine seals. Barometric pressure was measured at the surface and underground near the monitoring site since it was expected to be a contributor to variation in seal leakage rates. One method of analysis chosen for seal leakage rates utilised the application of the Atkinson equation [8]). In this way, changing pressure at a seal could be related to leakage or flow and seal resistance. This relationship could be described as linear or exponential based on the field data.

A second method of analysis included was a time series analysis to relate leakage rates to changes in barometric pressure that may not be site specific. Two accepted methods of time series analysis are the rescaled range technique [9,10] and the ARIMA approach, commonly referred to as the Box–Jenkins method [11,12].

Experimental design and study site

Mine study site

Field monitoring was conducted through a cooperative research agreement between Signal Peak Energy Bull Mountain No. 1 Mine operator and NIOSH. The monitored study site is shown in Figure 1, where the study panel is the one Right longwall panel measuring 380 by 4900 m (1250 by 16,000 ft). The mine operator had completed the first longwall panel and was mining the second when the study was performed. As with many western US coal mines, the mined coal seam has a relatively high spontaneous combustion potential. The mine began one Right longwall panel using a bleeder system but switched to bleederless system.

Ventilation description

An unusual feature of this mine is the application of an Australian Safety in Mines Testing and Research Station (SIMTARS) atmospheric monitoring system. The mine operator is working the thick Mammoth seam of relatively low-rank coal in the four corners region of Montana that is either of high-volatile bituminous C or sub bituminous coal rank. Due to the low rank of the mined coal, no methane is emitted from the coal bed with mining. Gas emissions from the mined seam consist entirely of carbon dioxide, although the gas present in the ventilation system may not be a ‘seam gas’ but could be a product of adjacent strata rock reactions or oxidation.

The underground monitoring site is shown in Figure 2. Entries are numbered from right to left in the figure. Instrument arrays were installed in entries 1 and 7 to produce data from the upwind and downwind sides of the seal line. Monitoring instrumentation consisted of a 0–25% oxygen sensor, a 0–5% methane sensor, a 0–3% carbon dioxide sensor, a digital flow metre, a digital barometer and a differential pressure monitor. With the exception of the differential pressure sensor and the barometer, an instrument array was installed on either end of the seal line. The differential pressure metre was installed on the number seven seal sampling line. The air sweeping the seal line was classified as intake air. Barometric pressure was measured at Entry 1 and differential pressure was measured at Entry 7.

Ventilation data analysis

Raw data consisted of measurements of data which were recorded every five minutes from 2:00 pm on 1 February through 12:20 pm on 17 May. In all but the final stage of analysis, data for the months of February and March, and for the months of April and May, respectively, were treated as two separate data-sets since it was thought that there could be some difference in the findings due to the change of season. Analysis of the monitoring data was conducted using two methods. The first is the Atkinson equation. The equation related leakage or flow quantity to head pressure, resistance and flow turbulence [13]. The Atkinson equation form used in the study is shown by the equation given below:

$$H_l = RQ^n$$

where H_l = head loss, R = resistance, Q = air quantity, n = exponent for quantity where n = 1 indicates laminar flow.

In fluid mechanics, H_l is shown to be proportional to Q^2 [8].

A second method of analysis used is a time series analysis. A time series is made up of observations of a variable made over time. The time interval between observations must remain constant throughout the series. Time units may be as small as minutes or as large as years. The purpose of time series analysis is to recognise the process or model underlying the observed data; identification of the model then makes it possible to forecast future observations.

After working with both statistical approaches, the classical method of time series analysis – the Box–Jenkins method – was chosen for this study [11,12] over the rescaled range technique [15]. The method uses four possible components of a time series: trend, seasonal cycles within a year, larger cycles over a period of one or more years and random error. One or more of these components is assumed to be present in every series. If only random error is present, then the observation at any given time point is considered to be independent of observations at previous time points, and no model can be identified. If in addition to random error, one or more of the other components is present, then the observation at any given time point is considered to be related to or influenced by observations at previous time point(s). The correlations between observations at a given time point and observations at an earlier time point are known as an ‘autocorrelations’.

The abbreviation for a Box–Jenkins model, ARIMA, stands for auto regressive (AR), integrated (I), moving average (MA) model. The term ‘integrated’ refers to the trend component. Theory holds that an observation at a given time point can be influenced either by the true value of an observation at a preceding time point (autoregressive), by the random error component of an observation at a preceding time point (moving average) or by both factors.

Results and discussion

Portions of the monitoring data are shown in Figure 3. The figure shows two weeks of differential pressure, barometric pressure at the surface and barometric pressure underground in Entry 1. The surface barometric pressure data were acquired at the instrumented monitoring trailer which included all of the SIMTARS instrumentation. The two barometric pressure measurement data-sets form lines with identical trends showing that the response of the underground ventilation system and instrumentation is essentially simultaneous with the atmospheric pressure changes occurring at the surface. The difference in pressure between the barometers is primarily attributable to differences in elevation between the monitoring sites and the ventilation pressure underground.

The differential pressure at the seal line varied from about 370 to 1100 pascals (1.5–4.4 in) of water gauge over the two-week data-set. A drop in barometric pressure is expected to correspond to an increase in seal differential pressure where the out-gassing from sealed areas in workings is promoted by the expansion of gases in the gob [16]. If this mechanism describes the correspondence between barometric and seal pressure, the data show that a discernible time lag occurs before the seal pressure response (Figure 3).

Prior research has shown cyclical patterns in barometric pressure data from surface monitoring sites including diurnal variations [6, 16]. No cyclicity was observed for two weeks of barometer data (Figure 3). One month of data was reviewed for the underground and surface measurements to further determine the presence or absence of the diurnal patterns of atmospheric pressure and no cyclicity was observed. It is not clear why the atmospheric pressure data from this study do not show diurnal cycles. However, the underground and surface data are shown to correspond well with each other at both the two-week and month scales.

A series of graphs were made to better understand the relationship between the amount of leaked gas flowing through the entry adjacent to the seals and barometric pressure to show any time lag associated with seal leakage rate. Leakage rates were calculated according to the method forwarded by Zipf and Mohammed [17]. Analyses were made of barometric pressure changes underground vs. the CO_2 quantity flowing adjacent to the seals, assuming delay intervals on hourly bases (1, 2, 3, 4, 5 h, etc.) Figure 4 shows a plot of CO_2 moving through the seals and into the adjacent entry vs. changes in barometric pressure measured underground for the plot that produced the best least squares fit to the hourly data. The figure shows February and March data using an 8-h delay between barometric pressure changes and CO_2 flow in the entry. The R^2 value for the quality of the linear fit to the data is about 0.75.

An evaluation of CO_2 volume in the entry sweeping the seals was performed to review their correspondence to barometric changes for the following two months of monitoring, April and May. The best linear fit to the data using the least squares method was achieved with a time lag of 10 h between barometric pressure changes and CO_2 flow in the entry. It was noted that the April–May barometric pressure changes showed more extreme variations in atmospheric pressure than the prior two months which displayed more short-term duration changes. This apparent change in atmospheric pressure behaviour may have resulted in the slightly longer time lag between barometric pressure changes and CO_2 flow in the entry. The No. 2 study panel had also retreated further in the last two months of monitoring, modifying the ventilation air path length. The R^2 value for the quality of the linear fit to the data is about 0.71. It is not clear why the April–May data produced lower R^2 values in linear fits to the data than the first two months, although prevailing weather patterns changed from winter to spring during this period, and changes in ventilation quantities are common as a panel retreats. The potential influence of seasonal weather patterns on barometric pressure patterns was a primary reason that the data-sets were viewed in separate, two-month groups.

To further investigate the relationship between seal leakage and differential pressure, the application of the Atkinson equation can provide some useful information. In the form of the equation shown, head or differential pressure is shown as a power function. For leakage of gas through a seal line, the magnitude of the exponent is an important variable in describing the relationship between the differential pressure and leakage rate. Figure 5 shows a plot of differential pressure on the seal line and seal leakage rate. A power curve trend line was fit to the data. The best-fit trend line in the form of a power curve gives an exponential value of about 0.69. The lower magnitude values appear to be primarily responsible for the concave down configuration of the trend line. The vertical alignment of points on the plot was produced by instrument measurement characteristics resulting in a high degree of scatter about some of the leakage rates. A linear trend was also fit to the data using the least squares method (not shown). The R^2 coefficient of determination calculated for both trends ranged from 0.85 to 0.86. Consequently, both trend lines support the concept of a linear relationship between H_l and Q and laminar flow through the seal.

Data from the second two months of monitoring were also plotted and analysed. A plot of differential pressure at the seal line and seal leakage rate was made where a power curve was fit to the data. The best fit to the data produced an exponential value of about 0.65 and an R^2 of about 0.71. A linear trend line (least squares method) fit to the data produced an R^2 of 0.70, showing the trend to be highly linear. Thus, the four months of monitoring data show that the exponent in the Atkinson equation is at or very near one, indicating laminar flow for the movement of air–gas mixtures out of the seal line in response to changes to differential pressure.

Time series analysis

Time series analysis was initially applied separately to the February–March and April–May data-sets. Due to the extremely large size of the full data-sets (more than 17,000 data points for February and March and more than 13,000 data points for April and May), reduced data-sets consisting of hourly measurements were used for analysis. It was felt that the use of the reduced data-sets would lessen the amount of noise and make patterns easier to identify. Hourly measurements were defined as the first measurement of every hour rather than as the average of the 12 measurements within every hour. Originally, the sets of data from February–March and April–May, respectively, were analysed separately. However, the sets were combined in the final analysis because of the similarity of results. A total of 14 hourly observations were missing because of power interruptions. Data for these time points were interpolated using statistical software produced by SAS [18].

The key parameters to be related by the time series analysis were barometric pressure and leakage rate to produce a model which would predict leakage rate based on barometric pressure data. During the analysis, it was shown that the output from the CO_2 concentration instrumentation used in the monitoring study produced a stepwise data trend at the leakage rates being measured (vertical groupings of data in Figures 5 and 6). The stepwise nature of the CO_2 concentration measurement instrumentation plot sufficiently modified the trend of CO_2 flow in the form of seal leakage data such that barometric pressure and leakage rate could not be meaningfully compared or modelled using time series techniques. The leakage of CO_2 was observed to trend well with differential pressure (Figure 6). Consequently, the two parameters used and compared for the time series analysis were barometric pressure and differential pressure.

As stated earlier in this paper, the influence of barometric pressure on the contraction and expansion of gases in mine gobs has been documented [16]. Therefore, time series analysis was used to meet two objectives: to describe the pattern of changes in barometric pressure over time, and to learn if changes in differential pressure at the mine seal were related to changes in barometric pressure.

A time series is a set of data collected on a single variable over a number of equally spaced time points. For example, data could be collected on temperature at a location every hour over a two-week period. The classical method of analysing a time series, the Box–Jenkins method, is used to uncover the model, i.e. pattern or process that explains the behaviour of the series. This method is based on the premise that the behaviour of a series can be explained by one or more of four components:

(1) Trend: general upward or downward movement over time.

(2) Seasonality: regularly occurring patterns over seasons of the year.

(3) Cyclicity: regularly occurring patterns over a period longer than one year.

(4) Random error: fluctuations that cannot be explained by any of the three previous.

The Box–Jenkins method proceeds by addressing the following questions in the order they are listed:

(1) Do changes over time reflect only random fluctuations or is there evidence that an underlying pattern of some type is present?

(2) If a pattern appears to be present, how can that pattern best be described or identified?

(3) How well does the identified pattern fit the observed data?

The examination of a plot of autocorrelations, known as a ‘correlogram’, is one of the key steps in the process. In the context of the current study, an autocorrelation quantifies the correlation between values of barometric pressure at different time points. A correlogram is a plot of autocorrelations at a succession of lags. The term 'lag' refers to the degree of separation in time. For example, the lag 1 autocorrelation is the correlation of observations at time points 2, 3, 4, 5, 6, 7, etc., with observations at time points 1, 2, 3, 4, 5, etc.

Barometric pressure data—Stationarity for a time series indicates that the mean and standard deviation do not change over the duration of the series [19]. A test for stationarity in the February–March data indicated the presence of a trend, and therefore, a plot using first differences was generated for trend removal. Figure 7 displays both the original series of barometric pressure data and the differenced series for trend removal.

Strong evidence of a pattern in barometric pressure was found. Results of the statistical analysis suggested that the pattern had three components. First, barometric pressure tended to increase over time (before trend removal). Second, the present value of barometric pressure was influenced by values at the two previous time points. Third, the present value of barometric pressure was influenced by the random fluctuation associated with the immediately preceding value. Statistical evidence showed that the identified model produced an adequate fit to the data. Although seasonal or cyclical variation in barometric pressure was observed in previous studies [6, 16], no evidence of cyclicity was found in the present study.

Relationship between barometric pressure and differential pressure

Cross-correlation analysis revealed that the strongest cross-correlations occurred at lag 0 and lag 1 (Figure 8). Each lag is equivalent to a 1–12 h time interval. A positive correlation is equal to a direct relationship between the two parameters; a negative correlation represents an inverse relationship between parameters. The correlation at lag 0 was negative (r = −0.542), whereas the correlation at lag 1 was positive (r = 0.686). The negative correlation at lag 0 implies that increases in Entry 1 barometric pressure tend to occur at the same time (an instantaneous response) as decreases in Entry 7 differential pressure, and vice versa. The strong positive lag 1 correlation implies that an increase in Entry 1 barometric pressure from time 1 to time 2 (for 12-h intervals) tends be followed by an increase in Entry 7 differential pressure from time 2 to time 3, and a decrease at Entry 1 tends to be followed by a decrease at Entry 7. Therefore, a change in Entry 1 barometric pressure can be helpful in predicting the direction of the next change in Entry 7 differential pressure.

The cross-correlation data agree with the observational and empirical data. With the mine seals outgassing essentially throughout the monitoring study, an increase in barometric pressure produced an immediate decrease in differential pressure at the seal line. This inverse relationship agrees with the lag 0 negative response in the cross-correlation analysis (Figure 8). After the initial response of the ventilation system to the barometric pressure change, the cross-correlation analysis shows that at lag 1, barometric pressure and differential pressure show a direct relationship and produce the highest r value of any 12-h lag period. This finding corresponds well to the empirical 8-h delay (Figure 4) and 10-h delay (April–May data-set) observed in the graphs of CO_2 flow and barometric pressure.

April–May data—As was the case for February and March, the barometric pressure and differential pressure data were found not to be stationary. The cross-correlation analysis revealed that the strongest cross-correlations occurred at lag 0 and lag 1 (Figure 9). Consistent with the results for February and March, the correlation at lag 0 was negative (r = −0.434), whereas the correlation at lag 1 was positive (r = 0.657). When Figure 9 is compared with Figure 8, the similarity in the pattern of cross correlations is evident. Because of the similarity in the results of cross-correlation analysis for the two time periods, the February–March and April–May data-sets were combined for the final analysis.

Predicting differential pressure from barometric pressure—A transfer function model was fit to estimate the equation for predicting Entry 7 differential pressure from Entry 1 pressure. All the coefficients in the model were statistically significant, and analysis of residuals showed that the model was adequate. Figure 10 displays a plot of observed and predicted values. The value of R^2 for the model was 0.45, indicating that almost half of the variation in Entry 7 differential pressure is explained by Entry 1 pressure. It can be concluded that Entry 1 pressure is an important determinant of Entry 7 differential pressure, but not the only determinant, since 55% of the variation is unexplained. The mine operator did perform ventilation changes over the monitoring period which is not accounted for in this analysis.

Summary and conclusions

The findings for this study are based on four months of mine monitoring data from the Signal Peak Energy Bull Mountain No. 1 Mine. The primary data-set for this study was underground monitoring data from a non-production section of the mine where intake air swept past a series of seven 340 kPa (50 psi) mine seals. The overall mine ventilation configuration during the monitoring period was that of a bleederless ventilation system with exhausting ventilation. The sealed, mined-out areas of the mine were designed be at a positive differential pressure relative to the active workings to produce a pattern of outgassing from the sealed areas to adjacent entries.

The monitoring effort included the measurement and recording of barometric pressure, differential pressure at the seal line, gas concentrations and airflow rates. The total amount of leakage through seven seals separating the mined-out gob from the active workings averaged 0.014 to 0.018 m^3/s (30–38 cfm) and ranged from 0 to 0.036 m^3/s (0–77 cfm). An empirical analysis of the monitoring data indicated that barometric pressure variations produced changes in seal leakage rates about 8–10 h later. Using the Atkinson equation, the change of leakage rates in response to differential pressure fluctuations was assessed. Both power curves and linear, least squares trends were fit to the data. The relationship between the two variables was found to be essentially linear. The power curve best fits to the data-produced exponents for Q of 0.69 and 0.65 for months 1 to 2 and months 3 to 4 of field measurements, respectively.

A time series analysis was done to relate barometric pressure data to differential pressure at the seal line. The ARIMA method produced results showing the potential for forecasting differential pressure at the seal line based on past barometric pressure measurements. The forecasting reproduced 45% of the measured data and yielded the patterns of differential pressure changes. Patterns in Entry 1 barometric pressure are not random; present observations are influenced by past observations. An equivalent way of interpreting statistical significance is to say that if observations were made over a four-month period at some future date, we would expect to see the influence of past observations on present observations again.

Since it was found that 45% of the variation over time in Entry 7 differential pressure could be explained by variation over time in Entry 1 barometric pressure, it can be concluded that the influence of Entry 1 barometric pressure is considerable. The statistical significance of the model provides evidence that the influence would be observed again if the study was repeated. However, since less than half of the variation is explained, forecasts of Entry 7 differential pressure made on the basis of Entry 1 pressure alone would not be highly accurate. Ventilation changes are known to have taken place during the four-month period of data collection near the monitored section, 1 South, which was not accounted for by these two parameters alone.

The response in leakage flow through mine seals has been shown to be essentially linear due to changes in atmospheric pressure. A mine operator could predict leakage rates through mine seals by conducting a monitoring study of atmospheric pressure, gas concentrations and flow rates at the seal lines. The curve of leakage flows through seals and atmospheric pressure can be used to predict flows at higher pressure changes than those observed. This relationship is expected to be site specific based on the R value of the seals and other localised factors (i.e. competency of adjacent rock, reservoir characteristics of adjacent rock, local atmospheric pressure patterns, etc.).

The time series analysis shows that barometric pressure determinations can be used to predict differential pressure at the seal line using the ARIMA model. This modelling approach was intended to be applicable to other mine sites but validation would be required. The findings here show that the atmospheric pressure measurements could be made either underground or at the surface since these measurements differed only by a constant. Cyclicity of barometric pressure patterns has been noted by other researchers. The removal of cycles from time series data can be performed but was not necessary in this study.

References

[1]. Gates RA, Phillips RL, Urosek JE, Stephan CR, Stoltz RT, Swentosky DJ, Harris GW, O'Donnell JR, Dresch RA. Fatal Underground Coal Mine Explosion. United States Department of Labor, Mine Safety and Health Administration, Coal Mine Safety and Health Report of Investigation. 2007 January 2, 2006, Sago Mine, Wolf Run Mining Company, Tallmansville, Upshur County, West Virginia, ID No. 46-08791.

[2]. Light TE, Herndon RC, Guley CE Jr. Cook CL Sr. Odum MA, Bates RM Jr. Schroeder ME, Campbell CD, Pruitt ME. Fatal Underground Coal Mine Explosion. United States Department of Labor, Mine Safety and Health Administration, Coal Mine Safety and Health Report of Investigation. 2007 May 20, 2006, Darby Mine No. 1, Kentucky, Darby LLC, Holmes Mill, Harlan County, Kentucky, ID No. 15-18185.

[3]. Zipf RK, Sapko MJ, Brune JF. Explosion Pressure Design Criteria for New Seals in U.S. Coal Mines. US Department of Health and Human Services, Public Health Service, Centers for Disease Control and Prevention, National Institute for Occupational Safety and Health. 2007:76. DHHS (NIOSH) Publication No. 2007-144, Information Circular No. 9500.

[4]. Sealing of Abandoned Areas Final Rule. 30 Code of Federal Regulations Part 75, Department of Labor, Mine Safety and Health Administration. US Government Printing Office; Washington, DC: 2007. Federal Register, Part III.

[5]. Weiss, ES.; Greninger, NB.; Stephan, CR.; Lipscomb, JR. USBM R.I. 1993. Strength Characteristics and Air-leakage Determinations for Alternative Mine Seal Designs; p. 9477

[6]. Hemp R. The effect of changes in barometric pressure on mines in the highveld of South Africa. J. S. Afr. Inst. Min. Metall. 1994; 94:133–146.

[7]. Cote, M.; Collins, R.; Pilcher, R.; Talkington, C.; Franklin, P. Methane Emissions from Abandoned Coal Mines in the United States: Emissions Inventory Methodology and 1990–2002 Estimates. 2004. EPA 430-R-04-001

[8]. Hartman, HL.; Mutmansky, JM.; Ramani, RV.; Wang, YJ. Mine Ventilation and Air Conditioning. 3rd ed.. Wiley; New York: 1997. p. 729

[9]. Chamoli A, Bansal AR, Dimri VP. Wavelet and rescaled range approach for the Hurst coefficient for short and long time series. Comput. Geosci. 2007; 33:83–93.

[10]. Pérez IA, Sánchez ML, García MA, Paredes V. Persistence analysis of CO_2 concentrations recorded at a rural site in the upper Spanish plateau. Atmos. Res. 2011; 100:45–50.

[11]. Hamilton, JD. Time Series Analysis. Princeton University Press; Princeton, NJ: 1994.

[12]. Enders, W. Applied Econometric Time Series. Wiley and Sons; Hoboken, NJ: 2010.

[13]. Montecinos, C.; Wallace, K. In: Hardcastle; McKinnon, editors. Equivalent roughness for pressure drop calculations in mine; 13th United States/North American Mine Ventilation Symposium; 2010. p. 225-230.

[14]. Zipf RK, Ochsner R, Krog R, Marchewka W, Valente M, Jensen R. Tube bundle system studies at Signal Peak Energy Bull Mountains #1 Mine. Trans. Soc. Min. Metall. Explor. 2013; 334:489–497.

[15]. Hurst HE. Long term storage capacities of reservoirs. Trans. Am. Soc. of Civ. Eng. 1951; 116:770.

[16]. Schatzel, SJ.; Krog, RB.; Dougherty, H. A field study of bleeder performance in US longwall coal mines; SME annual meeting and exhibition, Denver, CO, preprint 11–13; 2011. p. 7

[17]. Zipf, RK.; Mohamed, KM. In: Hardcastle; McKinnon, editors. Composition change model for sealed mine atmosphere in coal mines; 13th US/North American Mine Ventilation Symposium; Mirarco: 2010. p. 9

[18]. Milhøj, A. Practical Time Series Analysis Using SAS. SAS Institute Inc; Cary, NC: 2013.

[19]. Challis RE, Kitney RI. Biomedical signal processing. Part 2. The frequency transforms and their inter-relationships. Med. Biol. Eng. Comput. 1991; 29:1–17. [PubMed: 2016912]

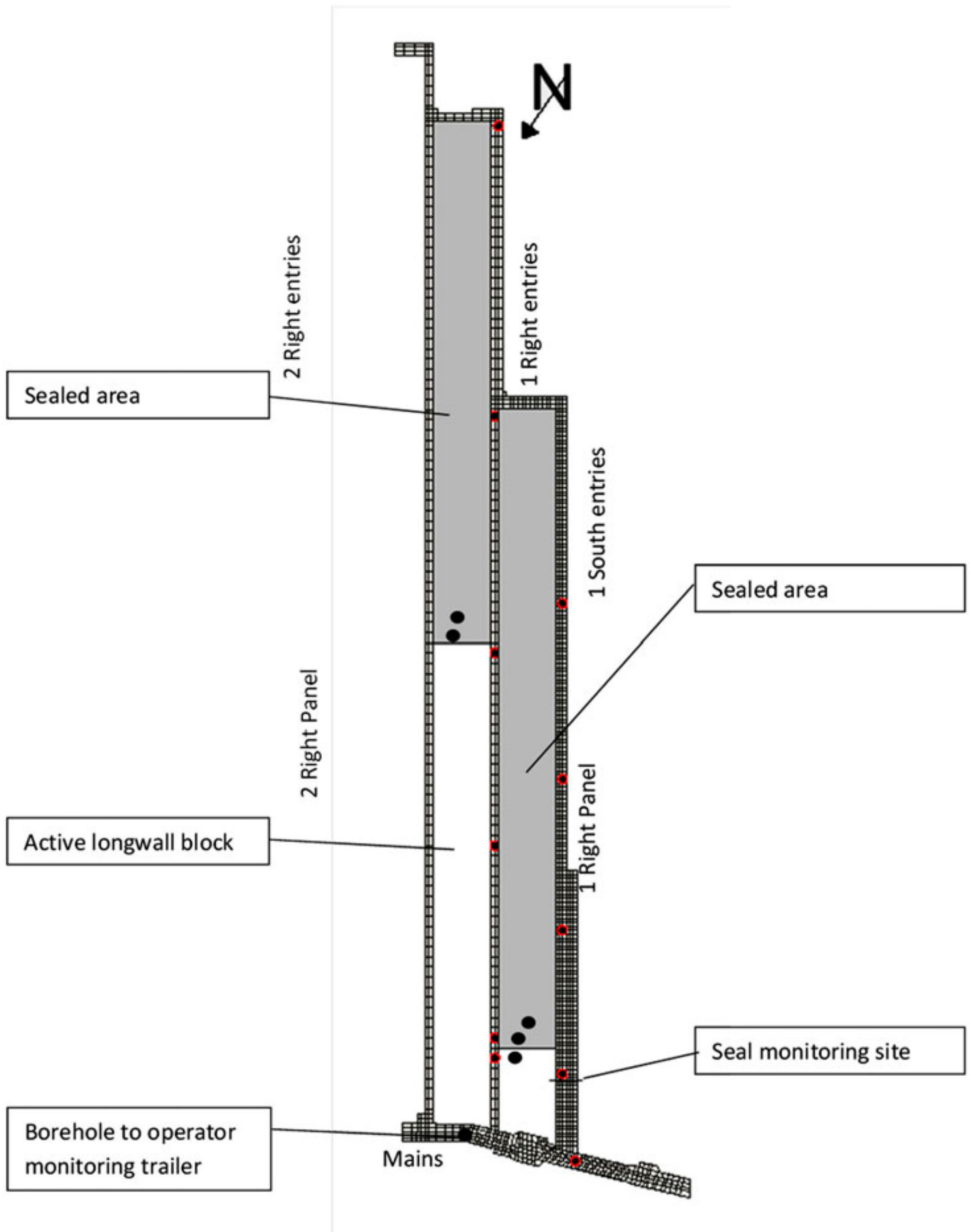

Figure 1.
Map of the Signal Peak Energy Bull Mountain #1 mine (modified from Zipf et al., 2013) [14].

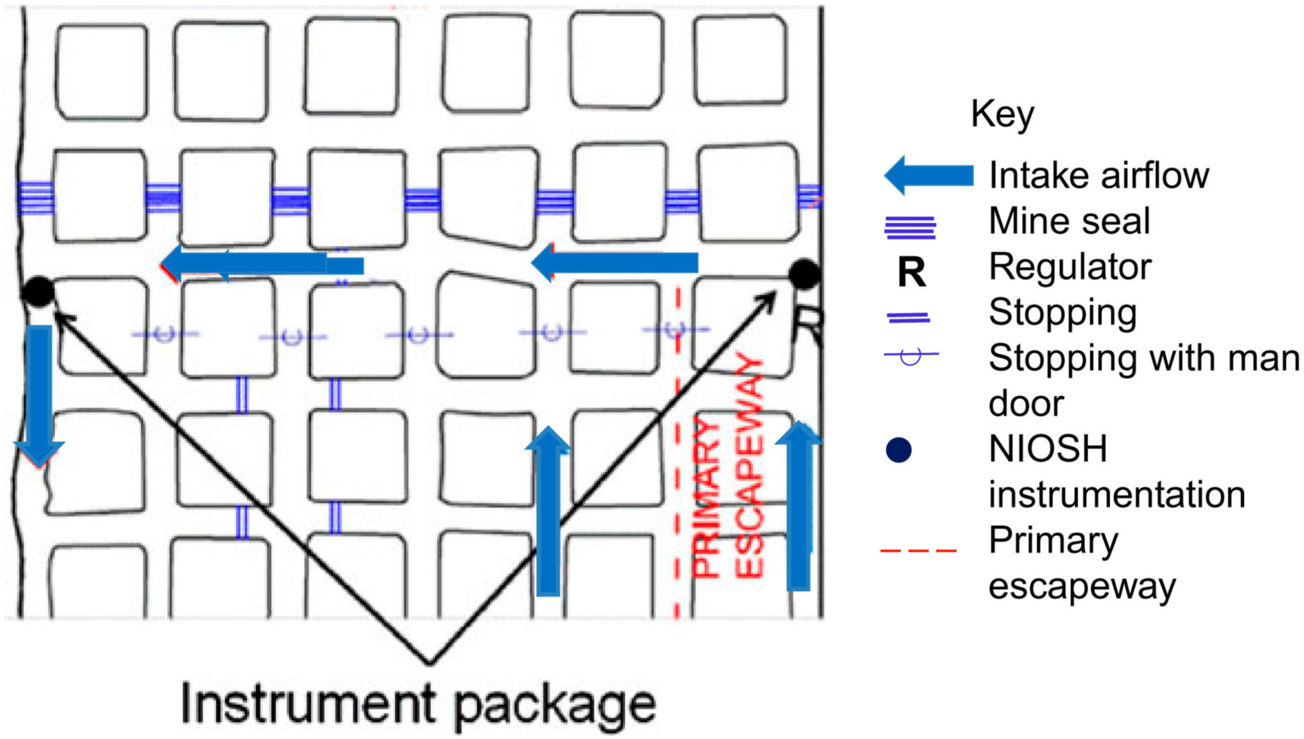

Figure 2.
Monitoring site for measurement of mine seal leakage rate.

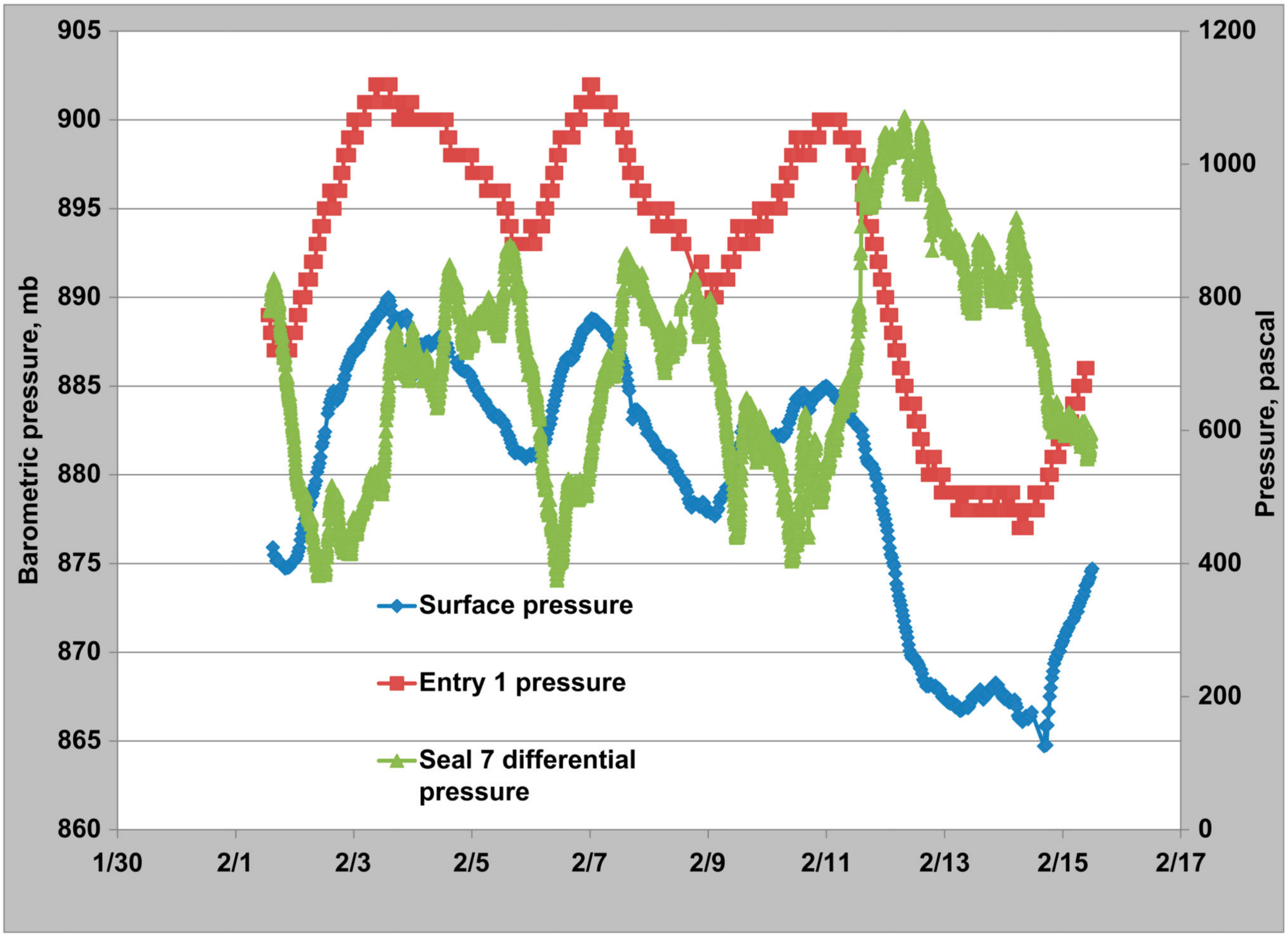

Figure 3.
Pressure changes measured underground and the surface at the mine study site.

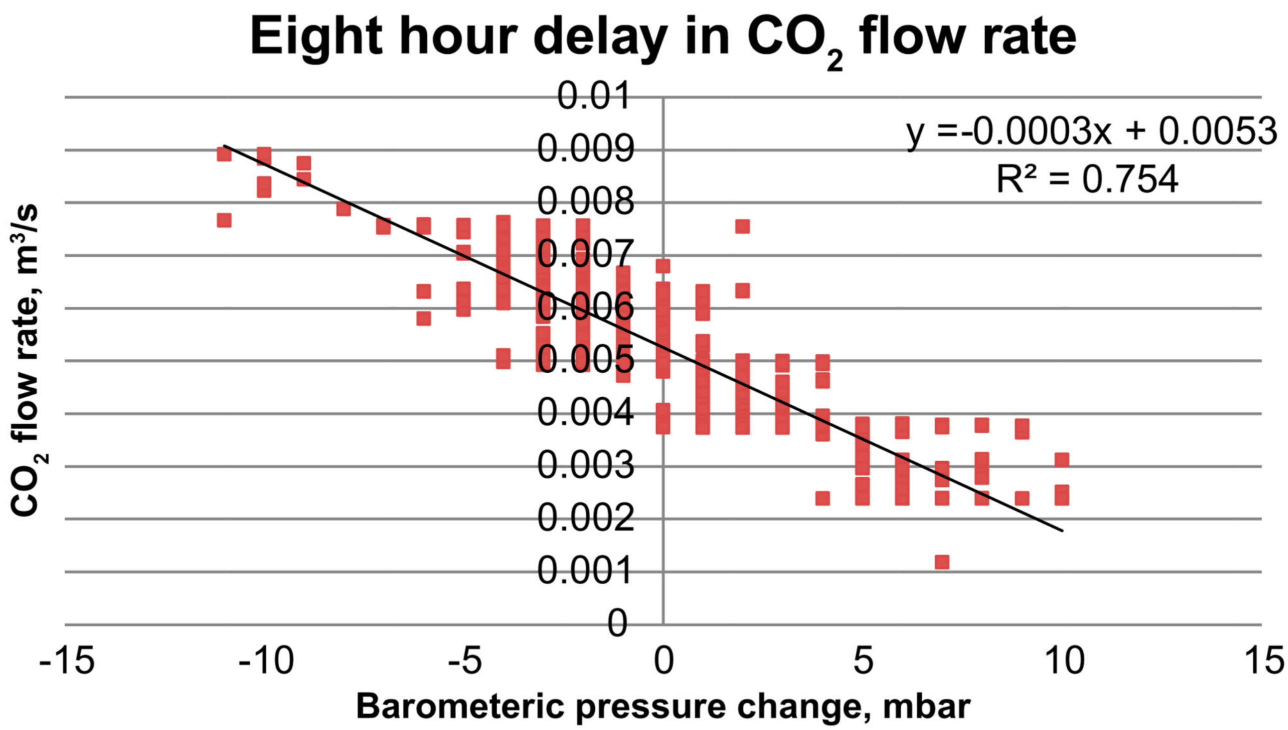

Figure 4.

Change in barometric pressure underground and CO_2 flow quantity through entries adjacent to mine seals, February and March.

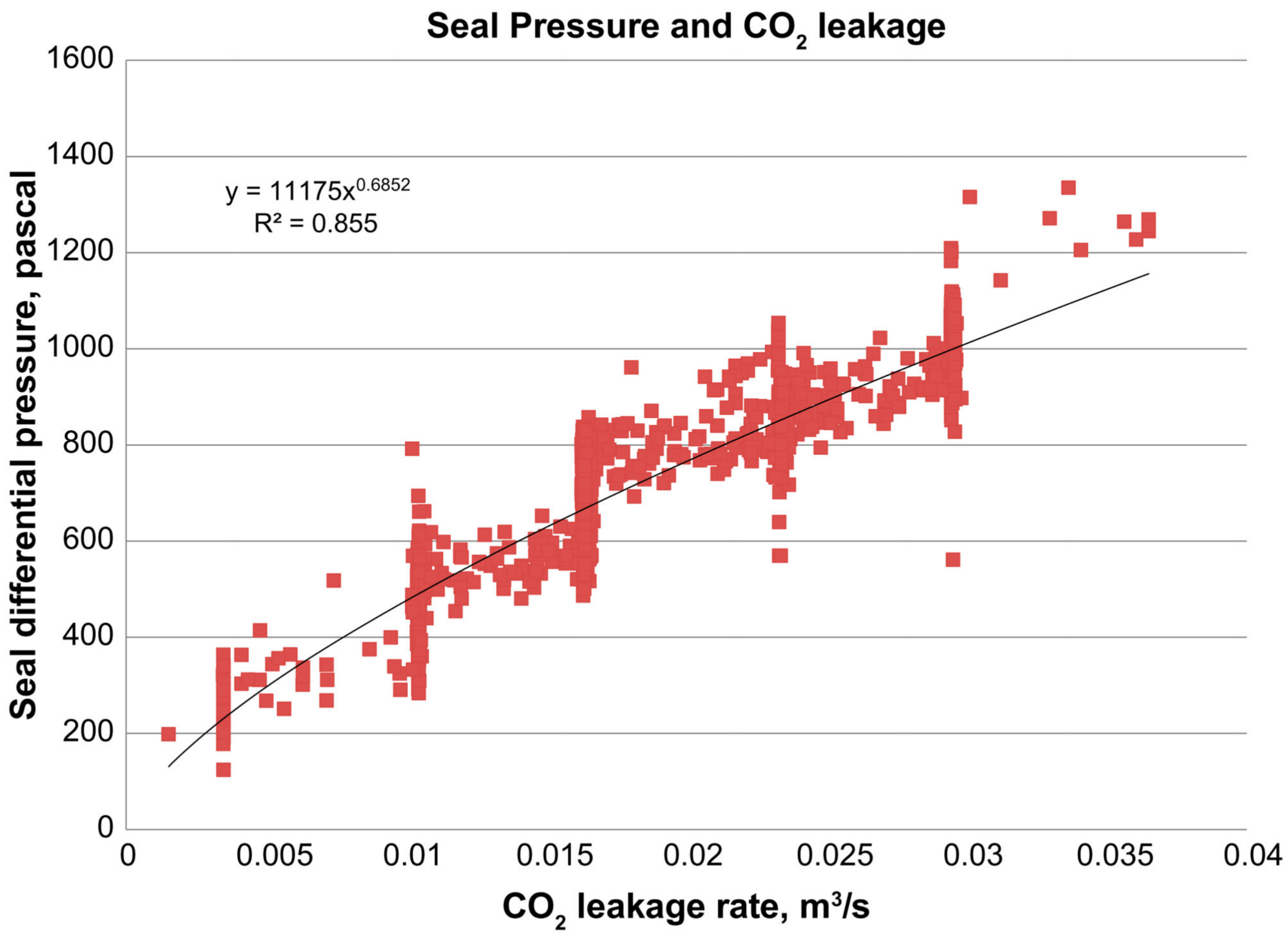

Figure 5.

Seal differential pressure and leakage rates, February and March. The figure also shows a power curve trend line fit to the monitoring data-set.

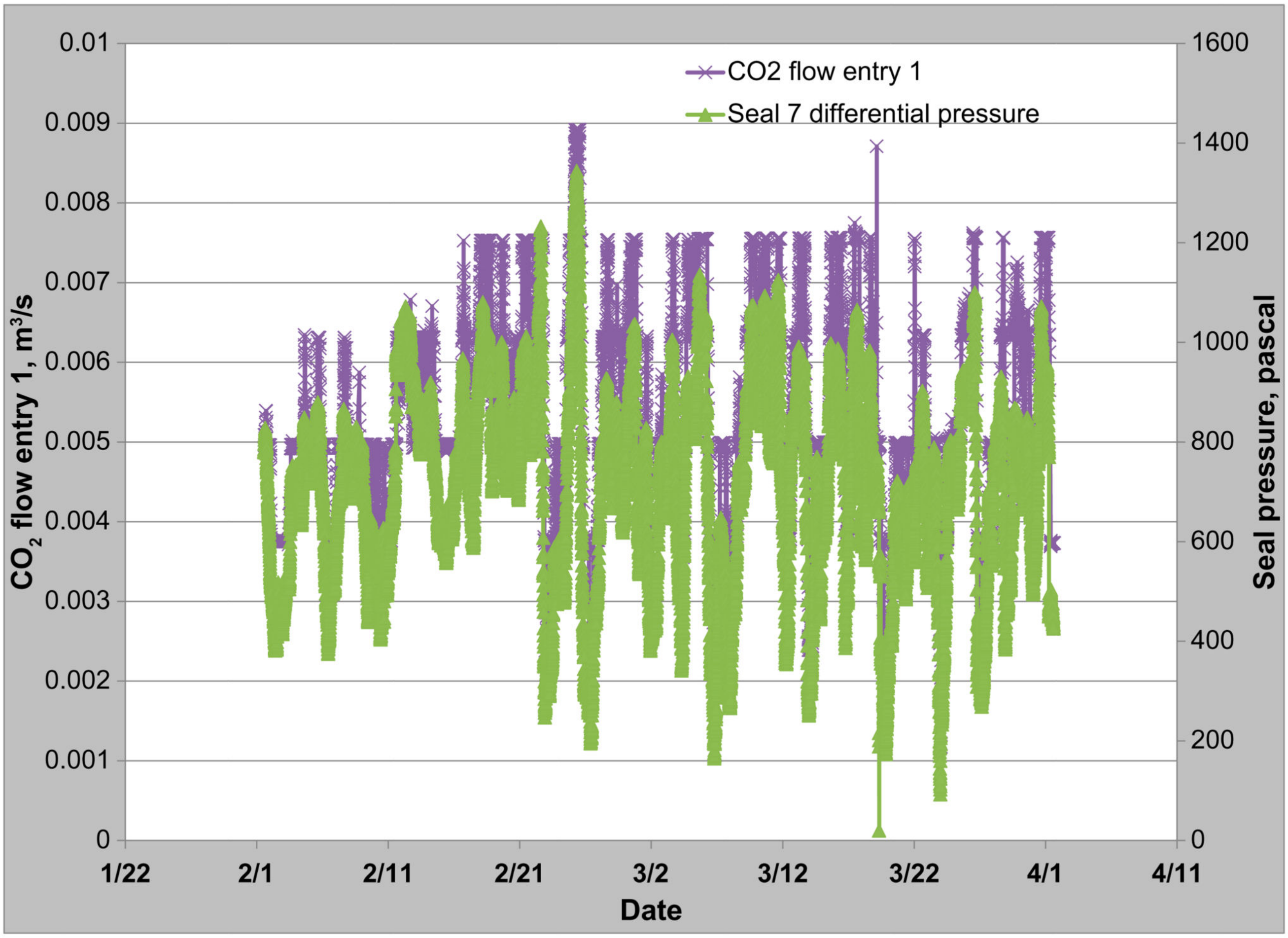

Figure 6.

Differential pressure and CO_2 flow in entry adjacent to seal line.

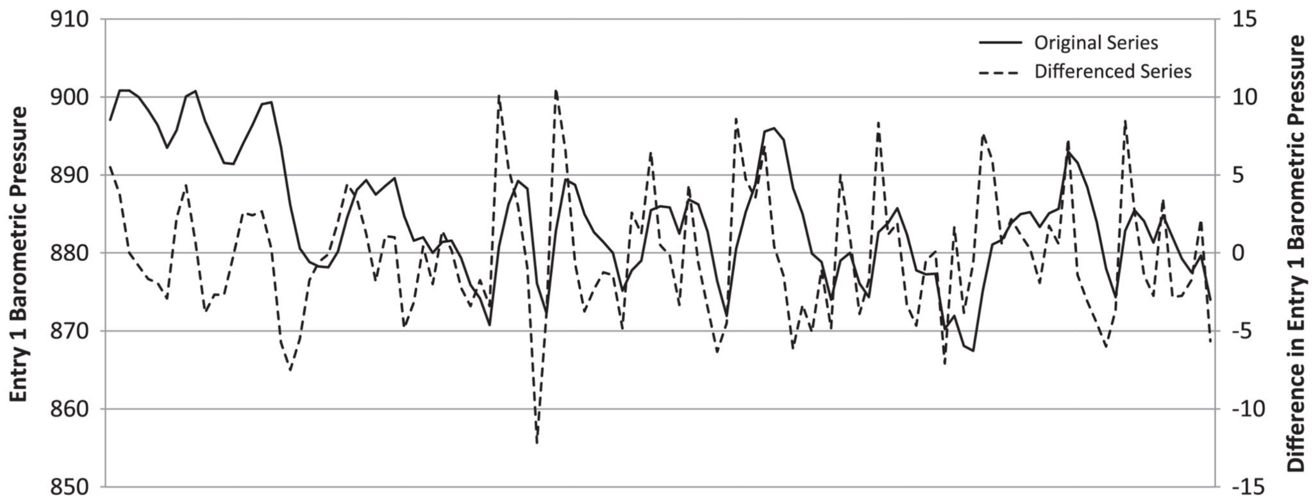

Figure 7.
Removing trends in barometric pressure data using 12-h plot intervals, February and March.

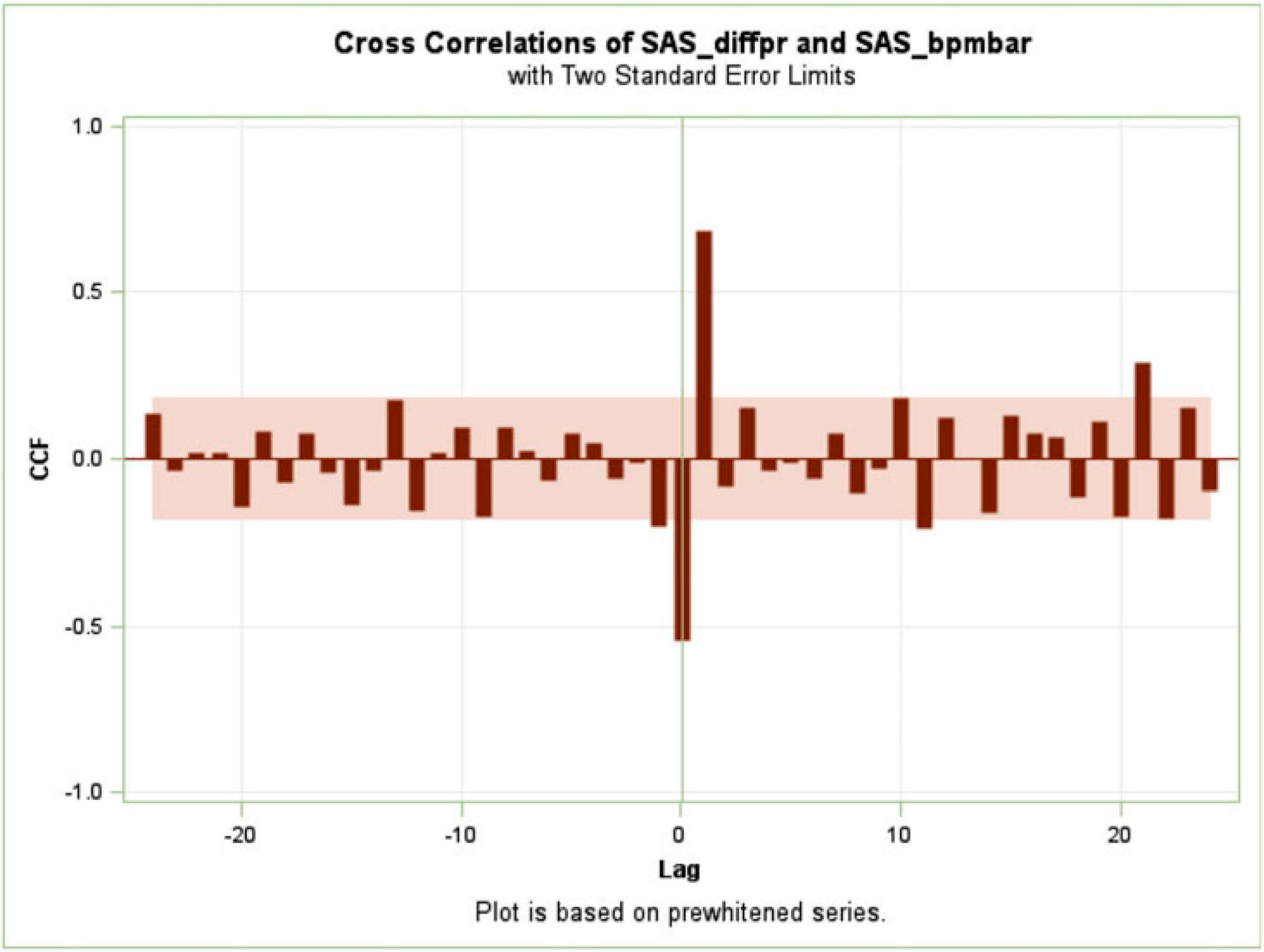

Figure 8.

Cross-correlation plots of barometric pressure and differential pressure for February and March.

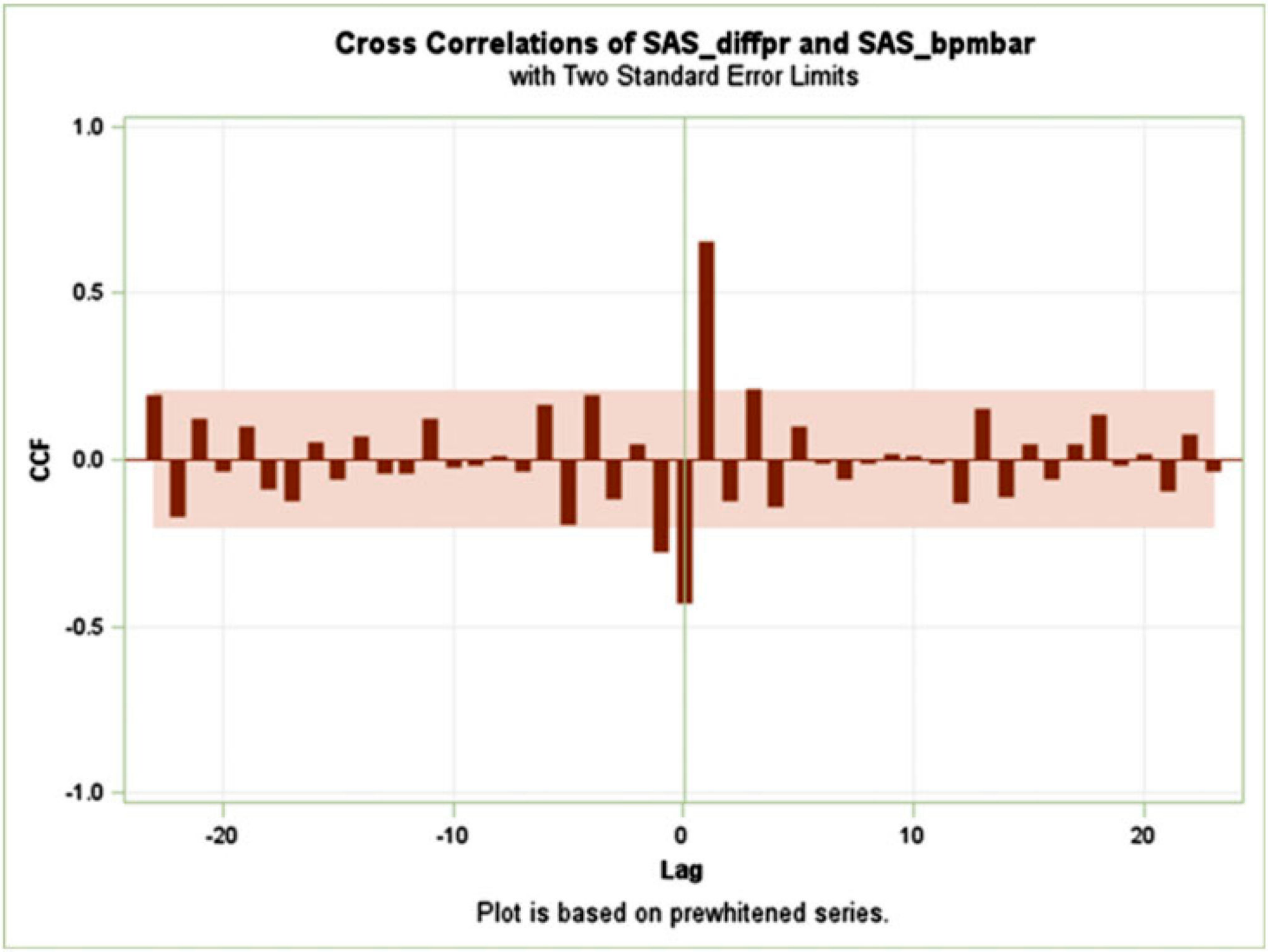

Figure 9.

Cross-correlation plots of barometric pressure and differential pressure for April and May.

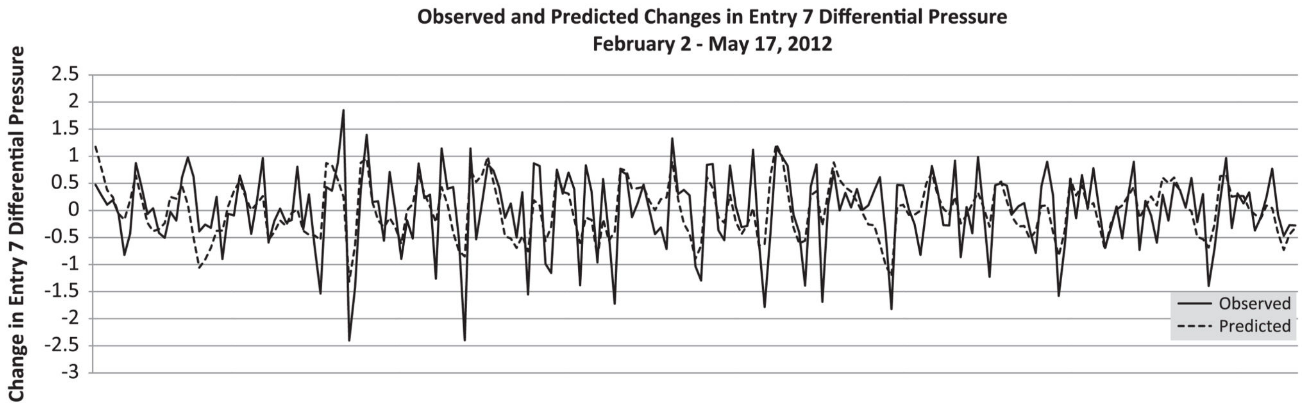

Figure 10.

Prediction of differential pressure at the seal line from barometric pressure data.